JCB Article

Disruption of cytoskeletal integrity impairs G_i-mediated signaling due to displacement of G_i proteins

Wilhelm Bloch,[1] Yun Fan,[2] Ji Han,[1] Sheng Xue,[2] Torsten Schöneberg,[3] Guanju Ji,[2] Zhong J. Lu,[2] Michael Walther,[1] Reinhard Fässler,[4] Jürgen Hescheler,[2] Klaus Addicks,[1] and Bernd K. Fleischmann[2]

[1]Institute of Anatomy I and [2]Institute of Neurophysiology, University of Cologne, Germany
[3]Institute of Pharmacology, Free University of Berlin, Germany
[4]Department of Experimental Pathology, University of Lund, Sweden

β1 integrins play a crucial role as cytoskeletal anchorage proteins. In this study, the coupling of the cytoskeleton and intracellular signaling pathways was investigated in β1 integrin deficient (−/−) embryonic stem cells. Muscarinic inhibition of the L-type Ca^{2+} current (I_{Ca}) and activation of the acetylcholine-activated K^+ current ($I_{K,ACh}$) was found to be absent in β1 integrin$^{-/-}$ cardiomyocytes. Conversely, β adrenoceptor-mediated modulation of I_{Ca} was unaffected by the absence of β1 integrins. This defect in muscarinic signaling was due to defective G protein coupling. This was supported by deconvolution microscopy, which demonstrated that G_i exhibited an atypical subcellular distribution in the β1 integrin$^{-/-}$ cardiomyocytes. A critical role of the cytoskeleton was further demonstrated using cytochalasin D, which displaced G_i and impaired muscarinic signaling. We conclude that cytoskeletal integrity is required for correct localization and function of G_i-associated signaling microdomains.

Introduction

Heart function, in particular the rhythm (chronotropy) and force of contraction (inotropy), is regulated by β-adrenoceptors and muscarinic type 2 (M2)* receptor–mediated activation/inhibition of L-type Ca^{2+} current (I_{Ca}) (chronotropy and inotropy) and acetylcholine-activated K^+ current ($I_{K,ACh}$) (chronotropy) (Sakmann et al., 1983). The signaling cascade involved in the modulation of I_{Ca} has been described in detail (for review see Trautwein and Hescheler, 1990). In vivo (Redfern et al., 1999) and in vitro studies have suggested that pertussis toxin sensitive G proteins of the G_i family mediate muscarinic depression of I_{Ca} (Wickman and Clapham, 1995; Ye et al., 1999; Chen et al., 2001) and activation of $I_{K,ACh}$ (Sowell et al., 1997). The involvement of NO in M2 receptor–mediated depression of I_{Ca} in adult heart is controversial (Han et al., 1998; Vandecasteele et al., 1999). We previously demonstrated that the mechanism of muscarinic regulation of I_{Ca} switches during embryonic development from a NO-mediated depression of basal I_{Ca} to direct G_i-mediated lowering of adenylyl cyclase (AC) activity in late stage cardiomyocytes (Ji et al., 1999).

Given that cytoskeleton-associated membrane receptors have been implicated in several heart disorders (for review see Towbin, 1998), we determined whether β1 integrin receptors modulate ionic conductances critical for heart function. Since β1 integrin$^{-/-}$ mice died shortly after implantation, chimeric mice or in vitro differentiated embryonic stem (ES) cell–derived β1 integrin$^{-/-}$ cells (Fassler et al., 1996) were used. Previous studies revealed several abnormalities in β1 integrin–deficient cells including migration and homing defects of haematopoietic cells (Hirsch et al., 1996), alterations in vasculo- and angiogenesis (Bloch et al., 1997), and severely disturbed cardiomyogenesis (Fassler et al., 1996). Although the biophysical characteristics of ionic conductances of β1 integrin$^{-/-}$ ES cell–derived cardiomyocytes appeared normal, the action potentials generated by deficient cardiomyocytes exhibited a primitive phenotype at all stages of differentiation (Fassler et al., 1996). Furthermore,

Address correspondence to B.K. Fleischmann, Institute of Neurophysiology, University of Cologne, Robert-Kochstr. 39, D-50931 Cologne, Germany. Tel.: 49-221-478-6940. Fax: 49-221-478-3834. E-mail: akp17@uni-koeln.de

Y. Fan, J. Han, and S. Xue contributed equally to this work.

*Abbreviations used in this paper: AC, adenylyl cyclase; CCh, carbachol; EB, embryoid body; EDS, early developmental stage; ES, embryonic stem; I_{Ca}, L-type Ca^{2+} current; $I_{K,ACh}$, acetylcholine-activated K^+ current; ISO, isoprenaline; I/V, current–voltage; LDS, late developmental stage; M2, muscarinic type 2; NOS, nitric oxide synthase; PDE, phosphodiesterase; PSF, point-spread function; wt, wild-type.

Key words: embryonic stem cells; signal transduction; ion channels; G proteins; β1 integrins

β1 integrin$^{-/-}$ ES cell–derived cardiomyocytes exhibited abnormalities in cytoskeletal integrity. Herein, we investigated the role of β1 integrins in hormonal regulation of I_{Ca} using β1 integrin$^{-/-}$ cardiomyocytes.

We report that β1 integrin$^{-/-}$ cardiomyocytes lacked muscarinic signaling, whereas β-adrenoceptor–mediated stimulation of I_{Ca} remained intact. This specific signaling defect was found to be related to spatial displacement of G proteins of the G_i-family.

Results

Muscarinic depression of basal I_{Ca} was found to be absent in β1 integrin$^{-/-}$ ES cell–derived cardiomyocytes

As previously reported (Ji et al., 1999), prominent inhibition (44.7 ± 8%; Fig. 1 d) of basal I_{Ca} density was observed upon application of the muscarinic agonist carbachol (CCh) (1 μM) (Fig. 1 a) in a large percentage of early developmental stage (EDS) cardiomyocytes (69%, $n = 13$; Fig. 1 c). Similarly, in the β1 integrin$^{+/-}$ ES cell–derived EDS cardiomyocytes, basal I_{Ca} density was depressed in half of the cells tested by 44 ± 8% ($n = 10$). In contrast, β1 integrin$^{-/-}$ cells did not exhibit CCh-mediated inhibition of basal I_{Ca} ($n = 37$) (Fig. 1, b, c, and e). To rule out that a shift in the voltage dependence of I_{Ca} underlies the CCh effect after the step to 0 mV, the current–voltage (I/V) relationship was defined in the presence and absence of CCh ($n = 5$). As depicted in Fig. 1 f, no CCh-mediated depression of I_{Ca} was observed at the chosen potentials.

β-adrenoceptor–mediated stimulation of I_{Ca} was preserved in β1 integrin$^{-/-}$ cardiomyocytes

The absence of muscarinic signaling could be explained by perturbed intracellular signaling components including AC, cAMP, or protein kinase A. Therefore, we determined whether additional regulatory pathways, and in particular the β-adrenoceptor–mediated stimulation of I_{Ca}, were defective in β1 integrin$^{-/-}$ cardiomyocytes. All wild-type (wt) late developmental stage (LDS) cardiomyocytes exhibited an increased current density (41.4 ± 6.8%, $n = 11$; Fig. 2, a and d) after prestimulation with the β-adrenoceptor agonist isoprenaline (ISO) (0.1 μM). Similarly, ISO increased the I_{Ca} density by 64.6 ± 12% ($n = 20$) in all β1 integrin$^{-/-}$ cardiomyocytes tested (Fig. 2, b and e). This ISO-induced upregulation of I_{Ca} was accompanied by a slight left shift in the I/V relationship ($n = 5$). However, superfusion with varying concentrations (1–10 μM) of CCh after β-adrenergic prestimulation did not suppress I_{Ca} in these cardiomyocytes ($n = 20$; Fig. 2, c and e). By contrast, CCh-inhibited ISO prestimulated I_{Ca} by 37.3 ± 7% ($n = 11$; Fig. 2 c) in 82% of wt LDS cells.

To address whether the signaling defect was caused by a quantitative reduction of muscarinic receptors, [^{3}H]QNB saturation binding studies were performed. There were no differences in the B_{max} values for β integrin$^{-/-}$ (33.7 ± 1.3 fmol/mg membrane protein) and wt ES cells (33.3 ± 3.1 fmol/mg membrane protein); therefore, a change in total muscarinic binding sites was excluded. Furthermore, immunocytochemical studies proved that $G\alpha_i$ is expressed in both, wt (Fig. 2 f) and β1 integrin$^{-/-}$ (Fig. 2 g) cardiomyocytes.

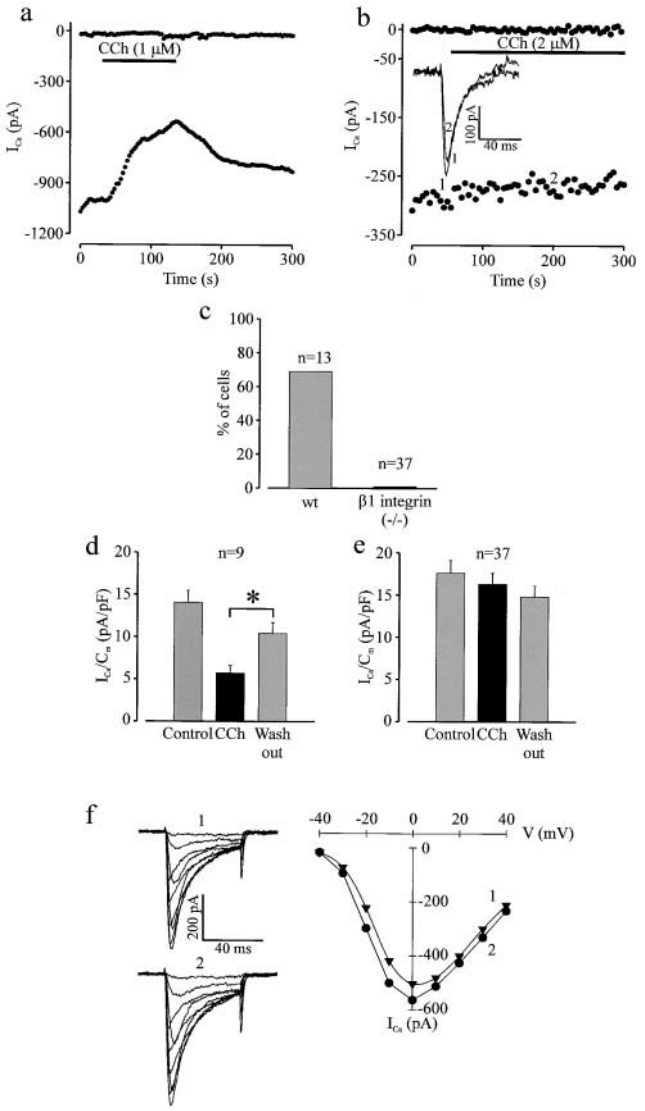

Figure 1. **Muscarinic modulation of basal I_{Ca} is absent in β1 integrin$^{-/-}$ ES cell–derived cardiomyocytes.** (a) Time course of peak I_{Ca} in a representative wt EDS ES cell–derived cardiomyocyte. Prominent inhibition of basal I_{Ca} was observed after application of carbachol (1 μM). The CCh effect could be reversed by washout. Each data point in the time course was evoked by a 20-ms depolarization from a holding potential of −50 mV to a test potential of 0 mV. The upper trace indicates the holding current. (b) A representative β1 integrin$^{-/-}$ EDS cardiomyocyte demonstrates the absence of the CCh-induced inhibition of basal I_{Ca} (50 ms depolarization from −50 mV to 0 mV). The time of current recordings (1 and 2, inset) is indicated. (c) Percentage of wt and β1 integrin$^{-/-}$ cardiomyocytes displaying CCh-induced inhibition of basal I_{Ca}. (d) I_{Ca} density in wt cells with CCh response. (e) I_{Ca} density in β1 integrin$^{-/-}$ cells in absence and presence of CCh. (f) Traces (left) and I/V relationship (right) of I_{Ca} recorded in an ES cell–derived EDS β1 integrin$^{-/-}$ cardiomyocyte (1, control; 2, in presence of CCh). I_{Ca} was evoked by 50-ms depolarizations from −40 mV to +40 mV in 10-mV increments (holding potential, −50 mV). *Indicates statistical significance (paired t test, p-value < 0.05).

Muscarinic signaling was restored in β1 integrin rescue ES cell–derived cardiomyocytes

To confirm that the muscarinic signaling defect was evoked specifically by the absence of the β1 integrin gene, we next investigated the hormonal modulation of I_{Ca} in β1 integrin rescue ES cell–derived cardiomyocytes. As depicted in Fig. 3 a, muscarinic receptor activation inhibited basal I_{Ca} by 32.3 ± 6% (Fig.

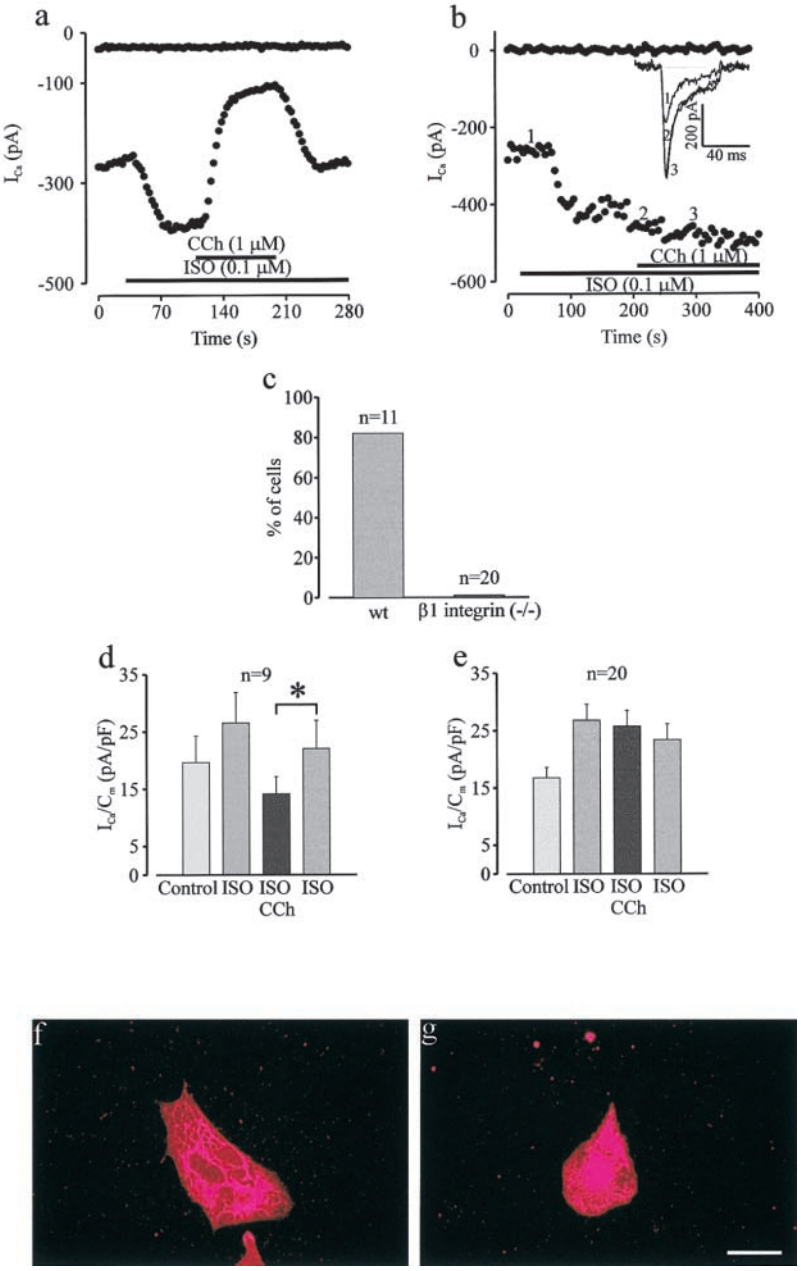

Figure 2. **Absence of muscarinic inhibition of ISO-prestimulated I_{Ca} in β1 integrin$^{-/-}$ ES cell–derived cardiomyocytes.** (a) I_{Ca} in a representative wt LDS ES cell–derived cardiomyocyte demonstrated prominent stimulation by ISO (0.1 μM) and subsequent inhibition by CCh. The CCh effect was reversed by ISO washout. (b) I_{Ca} in a representative β1 integrin$^{-/-}$ ES cell–derived LDS cardiomyocyte displayed strong stimulation by ISO; however, no inhibition by subsequent application of CCh was observed. (c) Percentage of wt and β1 integrin$^{-/-}$ cardiomyocytes displaying CCh-induced depression of ISO-prestimulated I_{Ca}. (d) I_{Ca} density in wt cells with ISO and CCh response. (e) I_{Ca} density in β1 integrin$^{-/-}$ cells exposed to ISO and CCh. (f–g) Immunostaining for $G\alpha_i$ expression in wt (f) and β1 integrin$^{-/-}$ ES cell–derived cardiomyocytes (g). *Indicates statistical significance (paired *t* test, p-value < 0.05). Bar, 25 μM.

3 d) in almost half (42%, $n = 19$; Fig. 3 d) of the EDS cells. In 36% ($n = 33$; Fig. 3 c) of the LDS β1 integrin rescue cardiomyocytes, CCh (1-10 μM) suppressed ISO prestimulated I_{Ca} by 21 ± 6% (Fig. 3, b and d). The reduction in muscarinic inhibition and altered morphology of β1 integrin reconstituted cells (see Fig. 5 i) suggests that the rescue was incomplete.

Hence, functional responses suggest that β1 integrin deletion resulted in a selective loss of muscarinic modulation of both, basal and ISO-prestimulated I_{Ca}, which could be restored upon reexpression of β1 integrins.

Nitric oxide and atrial natriuretic peptide–mediated depression of I_{Ca} is functionally intact in β1 integrin$^{-/-}$ cardiomyocytes

We next asked whether other signaling pathways involved in the regulation of I_{Ca} besides the β-adrenoceptor were affected by the β1 integrin deficit. Previous work in our group demonstrated constitutive nitric oxide synthase (NOS) 2 activity in EDS cells (Ji et al., 1999). Consistent with this observation, the NOS inhibitor *N*-methyl-L-arginine (L-NMMA, 0.2 mM) enhanced I_{Ca} by 30 ± 4% in the majority (75%, $n = 8$) of β1 integrin$^{-/-}$ EDS cells tested (Fig. 3 e). Similarly, as described for wt cardiomyocytes (Ji et al., 1999; Maltsev et al., 1999), application of the nonselective phosphodiesterase (PDE) inhibitor isobutylmethylxanthine (0.2 mM) increased the I_{Ca} density by 67.4 ± 7% ($n = 7$) in β1 integrin$^{-/-}$ EDS, and by 41.9 ± 7% ($n = 8$) in β1 integrin$^{-/-}$ LDS cardiomyocytes. The PDE2 subtype-specific antagonist erythro-9-(2-hydroxyl-3-nonyl)adenine (30 μM) also increased I_{Ca} density by 28.4 ± 5% ($n = 7$) in β1 integrin$^{-/-}$ EDS cardiomyocytes. Together, these findings demonstrate that these principal signaling cascades remained intact in β1 integrin$^{-/-}$ cardiomyocytes. By contrast to the missing CCh effect,

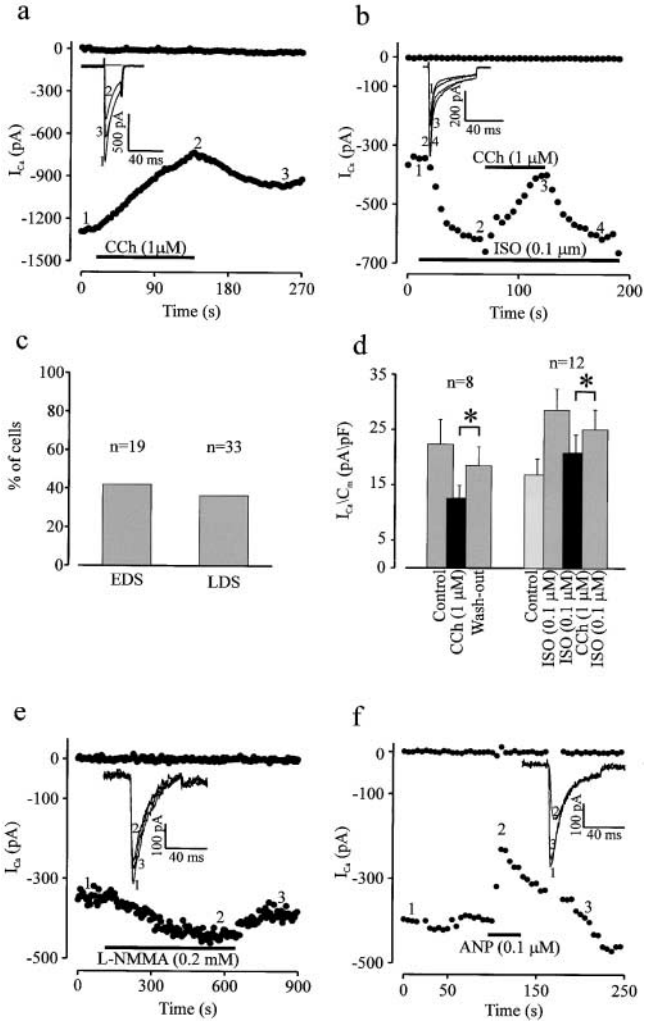

Figure 3. **Muscarinic modulation of I_{Ca} is restored in β1 integrin rescue ES cell–derived cardiomyocytes.** Other signaling cascades are intact in β1 integrin$^{-/-}$ ES cell–derived cardiomyocytes. (a) Basal I_{Ca} in a representative β1 integrin rescue EDS cardiomyocyte was inhibited by CCh. The CCh effect could be reversed by wash out. (b) ISO-prestimulated I_{Ca} in a representative β1 integrin rescue LDS cardiomyocyte was depressed by CCh. The CCh effect was reversed by ISO washout. (c) Percentage of β1 integrin rescue EDS and LDS cardiomyocytes responding to application of CCh or ISO and CCh. (d) Statistical analysis of I_{Ca} density in β1 integrin rescue EDS and LDS cardiomyocytes with CCh or ISO and CCh responses. (e) The NOS inhibitor L-NMMA (0.2 mM) augmented basal I_{Ca} in β1 integrin$^{-/-}$ EDS cardiomyocytes. This effect could be partially reversed by agonist wash out. (f) Atrial natriuretic peptide (ANP; 0.1 μM) induced a prominent depression of I_{Ca} in β1 integrin$^{-/-}$ LDS cells. *Indicates statistically significant difference (paired *t* test, p-value < 0.05).

atrial natriuretic peptide (ANP; rat fragment 3–28, 0.1 μM) depressed basal I_{Ca} density by 31.9 ± 3.9% ($n = 8$) in β1 integrin$^{-/-}$ cardiomyocytes (Fig. 3 f) as previously reported for wt ES cell–derived cardiomyocytes (Ji et al., 1999).

The defect in muscarinic signaling was found to reside at the G protein level

M2 receptor expression and key intracellular signaling cascades appeared intact in β1 integrin$^{-/-}$ cardiomyocytes. Therefore, we next examined whether the signaling defect was related to dysfunction of the pertussis toxin–sensitive G

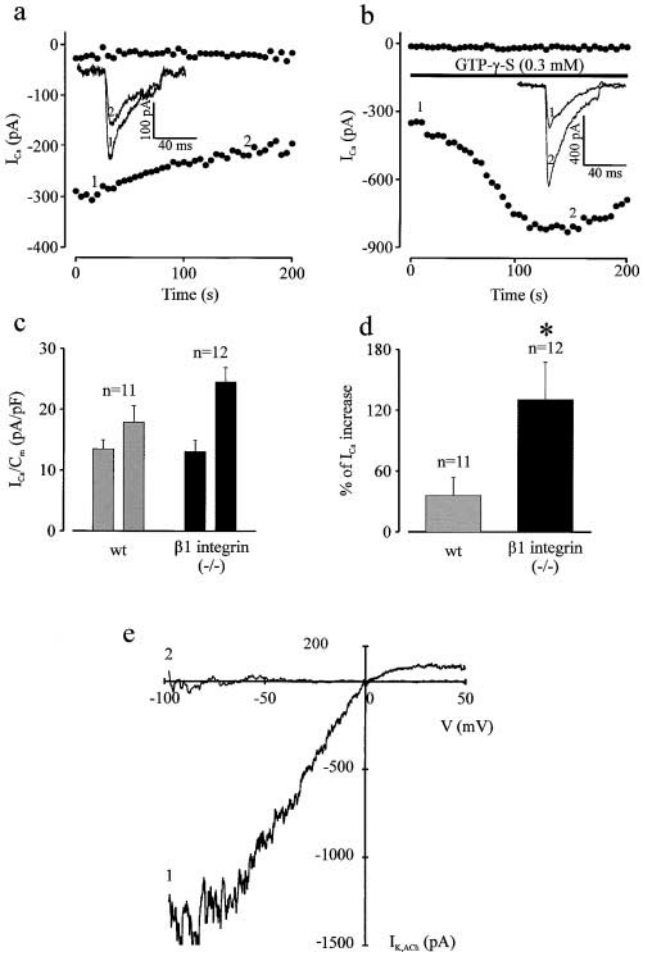

Figure 4. **Role of G proteins in the muscarinic signaling defect.** (a and b) Time course of peak I_{Ca} in a representative β1 integrin$^{-/-}$ LDS cardiomyocyte in the absence (a) or presence (b) of GTP-γ-S (0.3 mM) in the patch pipette. (c) Current density of control I_{Ca} after break in and upon maximal stimulation by GTP-γ-S in wt and β1 integrin$^{-/-}$ cardiomyocytes. (d) The percentage increase in I_{Ca} was significantly greater in the β1 integrin$^{-/-}$ cardiomyocytes. *Indicates statistically significant difference (unpaired *t* test, p-value < 0.05). (e) $I_{K,ACh}$ activation by GTP-γ-S (0.3 mM) was observed in a wt ES cell–derived cardiomyocyte (1) but not in a β1 integrin$^{-/-}$ cardiomyocyte (2). Representative background subtracted current ramp recordings are shown.

protein G_i. We previously reported that intracellular application of GTP-γ-S in guinea pig cardiomyocytes resulted in a slight stimulation of I_{Ca} (Hescheler et al., 1987), due to the opposing action of G_s and G_i proteins. Fig. 4 demonstrates that GTP-γ-S induced a small increase in I_{Ca} by 35.9 ± 18% ($n = 11$; Fig. 4, c and d) in wt LDS cardiomyocytes. Similarly, in integrin-reconstituted ES cell–derived cardiomyocytes, GTP-γ-S induced a small increase (46 ± 18.5%, $n = 4$) of I_{Ca} (data not shown). By contrast, GTP-γ-S caused a significant augmentation of I_{Ca} density (130.4 ± 37%, $n = 12$; Fig. 4, b–d) in β1 integrin$^{-/-}$ LDS cardiomyocytes that otherwise declined steadily in the absence of GTP-γ-S (Fig. 4 a). This suggests that the predominant action of GTP-γ-S is to activate G_s and that the β1 integrin-related signaling defect is due to a disturbance in G protein signaling.

Unlike adult cardiomyocytes, EDS and LDS cells did not respond to agonists of other G_i-coupled receptors including adenosine or somatostatin. Therefore, we used GTP-γ-S–

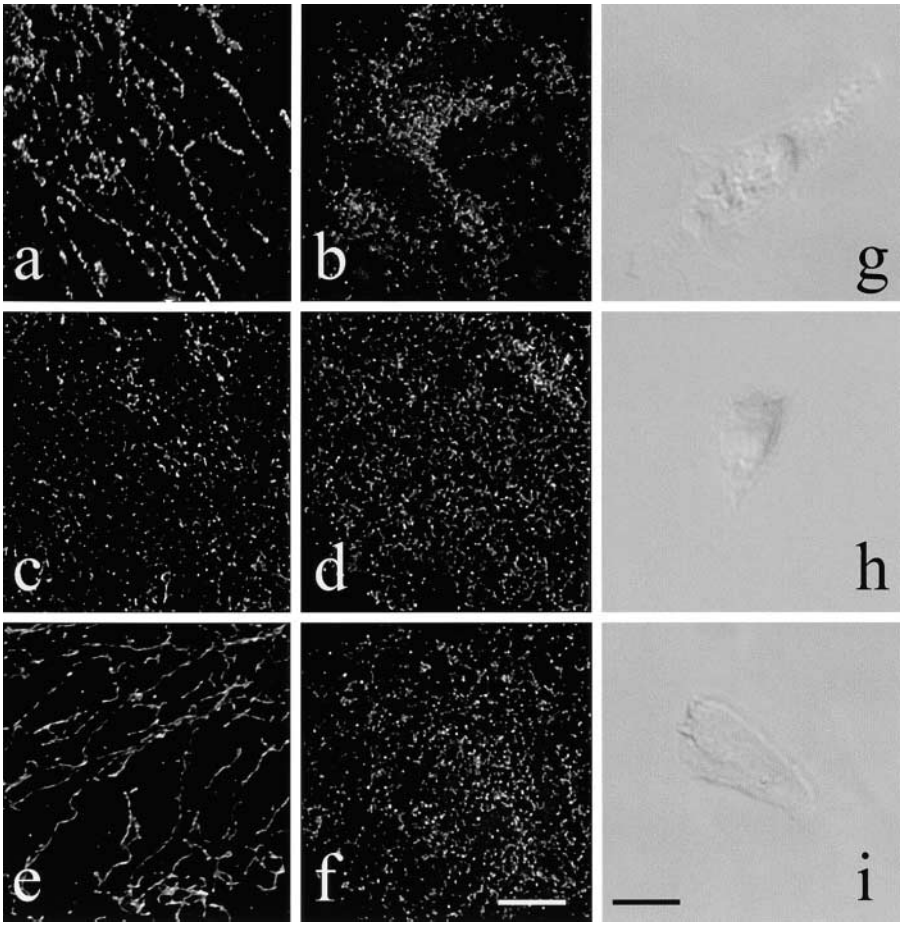

Figure 5. **Distribution pattern of $G\alpha_i$ in wt, β1 integrin$^{-/-}$, β1-integrin rescue, and cytochalasin D–treated cardiomyocytes.** (a, b, and f) Deconvolution microscopy was used to characterize the distribution pattern of $G\alpha_i$ in wt (a), β1 integrin$^{-/-}$ (b), and cytochalasin D–treated (10–20 μM for 4 h) cardiomyocytes (f). (e) Distribution of $G\alpha_i$ in β1 integrin rescue cardiomyocytes. (c and d) $G\alpha_s$ staining in wt (c) and β1 integrin$^{-/-}$ cardiomyocytes (d). (g, h, and i) DIC images of wt (g), β1 integrin$^{-/-}$ (h), and β1 integrin rescue (i) cardiomyocytes. Bars: (a–f) 5 μm; (g–i) 25 μm.

mediated activation of $I_{K,ACh}$ to examine G_i-coupling pathways. Although $I_{K,ACh}$ could be activated in wt ($n = 14$) and β1 integrin rescue cells ($n = 4$, data not shown), no GTP-γ-S–evoked activation of $I_{K,ACh}$ could be observed in β1 integrin$^{-/-}$ cardiomyocytes ($n = 14$), consistent with the effect on I_{Ca} regulation.

$G\alpha_i$ distribution is altered in β1 integrin$^{-/-}$ ES cell–derived cardiomyocytes

Immunostaining was used to investigate the patterns of G protein expression. Antibodies against G_α subunits were used because of the large number of possible β and γ subunits that could be involved in receptor coupling. Differences in the cellular distribution of $G\alpha_i$ and $G\alpha_s$, $G\alpha_o$, the M2 receptor, and L-type Ca^{2+} channels (VDCC) (data not shown) were found in wt cells. The vast majority of murine embryonic (68.2 ± 11.7%, $n = 489$) and wt ES cell–derived (64.0 ± 24.0%, $n = 210$) cardiomyocytes displayed a network-like pattern of $G\alpha_i$ expression, whereas relatively few (20.8 ± 3.6%, $n = 441$) β1 integrin$^{-/-}$ cardiomyocytes displayed this pattern. Consistent with this finding, nearly all cells in whole embryoid bodies (EBs) (90.8 ± 7.9%, $n =$ 1,000, five experiments) exhibited a linear network-like distribution pattern of $G\alpha_i$ expression, whereas few (10.5 ± 6.1%, $n = 800$, 4 experiments) β1 integrin$^{-/-}$ EBs had this pattern.

We next investigated the subcellular distribution of these G proteins at higher resolution using deconvolution microscopy. Cardiomyocytes, which were identified by α-actinin staining (Kolossov et al., 1998), exhibited a linear- and network-like distribution pattern of $G\alpha_i$ in wt (Fig. 5 a) cells and diffuse staining of $G\alpha_s$ in the wt (Fig. 5 c) cells. β1 integrin$^{-/-}$ ES cell–derived cardiomyocytes exhibited diffuse staining for $G\alpha_i$ (Fig. 5 b) and $G\alpha_s$ (Fig. 5 d). Consistent with our functional results, a network-like distribution was also observed in the β1 integrin rescue cells (Fig. 5 e), whereas $G\alpha_o$ was diffusely distributed throughout all cells (data not shown). In addition to distinct patterns of $G\alpha_i$ distribution, β1 integrin$^{-/-}$ ES cell–derived cardiomyocytes had different shapes as compared with the wt (Fig. 5, g and h) (Fassler et al., 1996). β1 integrin rescue cells showed a partial morphological reversal (Fig. 5 i).

Together, these findings are consistent with the electrophysiological results, which suggest that G_i underlies the muscarinic signaling defect.

$G\alpha_i$ colocalizes with focal contact proteins

A similar network-like distribution of $G\alpha_i$ has been reported for β1 integrin focal adhesion–associated molecules such as talin and vinculin (Kostin et al., 1998; Imanaka-Yoshida et al., 1999). We have identified a unique architecture for $G\alpha_i$ in the β1 integrin$^{-/-}$ cells and found that talin and vinculin exhibit a similar diffuse distribution as $G\alpha_i$ (data not shown). We subsequently analyzed the interaction between β1 integrins, talin, and vinculin with $G\alpha_i$ using deconvolution and electron microscopy. These approaches failed to demonstrate a close colocalization of β1 integrins and $G\alpha_i$ (Fig. 6 a). Deconvolution microscopy did reveal, however,

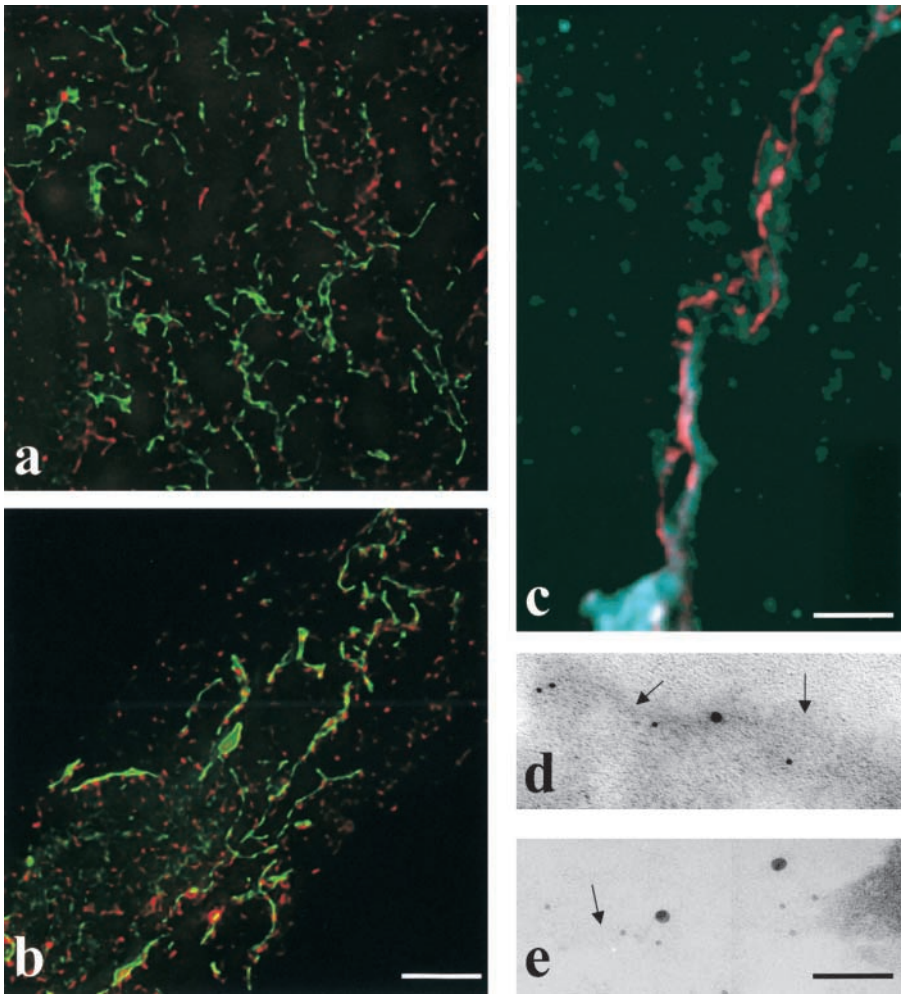

Figure 6. **$G\alpha_i$, talin, and vinculin colocalize in wt cells.** (a and b) Deconvolution microscopy of ES cell–derived cells exhibited no overlap of $G\alpha_i$ and β1 integrins (a), but colocalization of $G\alpha_i$ and talin (b). (c) Higher magnification showing colocalization of $G\alpha_i$ and talin. (d and e) Immunogold staining for $G\alpha_i$ and vinculin in murine embryonic cardiomyocytes (d) and in adult mouse heart (e). Vinculin and $G\alpha_i$ were labeled with 5- and 15-nm gold particles, respectively. The distance between pairs of gold particles was 40–150 nm. Bars: (a and b) 6 μm; (c) 2.5 μm; (d and e) 90 nm.

spatial colocalization between $G\alpha_i$ and both vinculin and talin (Fig. 6, b and c) in wt cells. Electron microscopy of double immunogold–labeled cells further revealed a relatively close colocalization between $G\alpha_i$ and vinculin (40–150 nm) in embryonic (Fig. 6 d) and adult mouse/rat cardiomyocytes (Fig. 6 e), suggesting that direct protein–protein interaction is highly unlikely.

Cytochalasin D recapitulates the functional and morphological changes induced by β1 integrin deficiency

To further test whether muscarinic signaling is dependent on the integrity of the cytoskeleton, isolated murine embryonic cardiomyocytes (E11.5, E17.5) were incubated with cytochalasin D (10–20 μM) to immobilize the cytoskeleton. Cytochalasin D–treated cardiomyocytes (E11.5) displayed fast run down of I_{Ca}, and the majority (85.7%) of cells tested were unresponsive to CCh ($n = 21$). By contrast, CCh depressed basal I_{Ca} by 45.7 ± 3% ($n = 5$) in 60% of untreated cells. ISO-mediated stimulation of I_{Ca} remained intact in cytochalasin D pretreated murine cardiomyocytes ($n = 5$, E17.5). Cytochalasin D treatment also induced a diffuse distribution of $G\alpha_i$ in both, ES cell–derived cells and murine embryonic cardiomyocytes (Fig. 5 f), consistent with the pattern observed in the β1 integrin$^{-/-}$ cardiomyocytes.

Discussion

In this study, we provide evidence that β1 integrin deletion results in a selective loss of muscarinic signaling in cardiomyocytes. This signaling defect is clearly related to the lack of β1 integrins because reconstitution with β1 integrins reversed the altered morphology and the muscarinic signaling in β1 integrin$^{-/-}$ ES cells.

Evidence for G_i dysfunction in β1 integrin$^{-/-}$ cardiomyocytes

To date, β integrins have been shown to play an important role primarily in tyrosine kinase–mediated signaling (see for review Ruoslahti, 1997). Furthermore, integrin-dependent cell anchorage regulates the efficiency of signaling from G protein–coupled receptors (Short et al., 2000). In β1 integrin$^{-/-}$ cardiomyocytes, except for an absence of muscarinic regulation of I_{Ca} and $I_{K,ACh}$, no other signaling defects could be detected. Our functional data pinpoint the signaling defect at the level of G_i, as intracellular dialysis with GTP-γ-S resulted in pronounced enhancement of G_s-mediated stimulation of I_{Ca} and defective activation of $I_{K,ACh}$ in the β1 integrin$^{-/-}$ cardiomyocytes. In previous investigations, antibody neturalization of integrins in situ revealed a role for integrins in the modulation of I_{Ca} or I_{Ba} (Wu et al., 1998). A recent study found that cat cardiomyocytes cultured on laminin-coated cover slips had disturbed cholin-

ergic and β-adrenergic responses (Wang et al., 2000a,b). These data are consistent with our findings and indicate a critical role for integrins in both receptor coupling and ion channel modulation. Clark et al. (1998) suggested that changes in integrin matrix interactions might underlie defects in signaling molecule clustering. Herein, we provide mechanistic evidence that receptor expression remains unchanged upon β1 integrin deletion; however, the altered distribution pattern of G_i proteins is observed only under conditions that also result in a muscarinic signaling defect.

Role of the cytoskeleton in G protein function

Our work also demonstrates a focal adhesion–related intracellular distribution for $G\alpha_i$, but not $G\alpha_s$, and $G\alpha_o$. The idea that components of the cytoskeleton can determine G protein localization and function (for review see Janmey, 1998) has been proposed before by Ueda et al. (1997) and Ibarrondo et al. (1995) who found a direct association between the γ12 subunit and between $G\alpha_q$/$G\alpha_{11}$ and actin filaments, respectively. Furthermore, the activation and release of $G\alpha_{i2}$ from the cytoskeleton has been reported (Sarndahl et al., 1996). Consistent with our functional findings, the subcellular distribution of $G\alpha_i$ was severely altered by the β1 integrin deficiency in cardiomyocytes. Our findings are also consistent with previous studies using antisense approaches (Kleuss et al., 1991, 1993), where, in contrast to G protein knock-out models (Rudolph et al., 1996), selective G protein–mediated receptor–effector coupling could not be reconstituted at all by other G proteins. This is also supported by recent work, where selective G protein β/γ complexes were shown to be involved in the inhibition of neuronal Ca^{2+} channels (Diverse-Pierluissi et al., 2000). This study suggests that the specificity of signal transduction is not only related to protein–protein interaction, but also to the spatial arrangement of signaling components.

Due to the similar cellular distribution observed for $G\alpha_i$ and that reported for the focal contact–associated proteins talin and vinculin, we tested their spatial relation to one another in cardiomyocytes. In wt cardiomyocytes, $G\alpha_i$ and both talin and vinculin colocalized, whereas they did not in β1 integrin$^{-/-}$ cardiomyocytes. The association between these molecules was further demonstrated by inhibiting the polymerization of G actin to F actin with cytochalasin D (Vasioukhin et al., 2000), which resulted in a similar alteration in cellular morphology and signaling, as observed in β1 integrin$^{-/-}$ cells.

The parallel relationship between cellular structure and function that we observe in cardiomyocytes suggests that β1 integrins play an important role in organizing the spatial association between signaling molecules such as G_i and focal adhesion–associated proteins. A similar relationship was demonstrated for caveolin (Anderson, 1998) and PDZ domains (Fanning and Anderson, 1999). It was proposed that anchoring proteins of the PSD-95/SAP90 family are required for G protein stimulation of the membrane-associated synaptic ion channel Kir3.2c (Hibino et al., 2000). An important role of signaling microdomains in cardiomyocytes has been demonstrated by Jurevicius and Fischmeister (1996), who demonstrated that colocalization of AC/cAMP and PDEs leads to a tight regulated local control of the ISO-mediated upregulation of I_{Ca}.

Thus, we propose that β1 integrin deletion results in altered cytoskeletal architecture due to the loss of important anchorage proteins. This causes spatial displacement of G_i proteins and both a physical and functional disruption of signaling microdomains.

Materials and methods

ES cell preparation

Studies used ES cells of the D3 line (wt) (Doetschman et al., 1985; Wobus et al., 1991), the heterozygous β1 integrin$^{+/-}$ ES cell line, the β1 integrin$^{-/-}$ ES cell line generated on D3 background (Fassler et al., 1995), and the β1 integrin rescue ES cell line. This line was generated by reexpressing β1 integrins in β1 integrin$^{-/-}$ ES cells under control of the phosphoglycerate kinase promoter. wt and β1 integrin$^{+/-}$ ES cells were cultured and differentiated into spontaneously beating cardiomyocytes as previously described (Wobus et al., 1991). EDS cells were derived from EBs plated for 3–4 d and LDS cells from EBs 9–12 d after plating. β1 integrin$^{-/-}$ and β1 integrin rescue ES cells were grown on gelatin-coated cover slips without feeder cells in medium supplemented with 5 ng/ml recombinant human leukemia inhibitory factor (Fassler et al., 1996). β1 integrin$^{-/-}$ ES cells were cultured for 3 d in hanging drops and 3 d in suspension before plating on gelatin-coated plates. Because of the delayed onset of beating, β1 integrin$^{-/-}$ cardiomyocytes derived from EBs plated for 6–10 d were defined as EDS, and those cultured for 14–18 d were defined as LDS cells (Fassler et al., 1996). β1 integrin rescue ES cells were maintained in presence of G418 (300 μg/ml). Single cardiomyocytes were isolated from clusters of spontaneously beating areas as previously described (Ji et al., 1999). Murine embryonic (E11.5, E17.5) ventricular cardiomyocytes were harvested from superovulated mice (Fleischmann et al., 1998). The heart was removed from the embryo, and the cardiomyocytes were isolated by collagenase digestion.

Cytochalasin D treatment

~12 h after dissociation, murine embryonic cardiomyocytes were treated with cytochalasin D for times indicated (15 min–16.5 h). Murine embryonic cells were incubated with 10 μM cytochalasin D and ES cell–derived cardiomyocytes with 20 μM cytochalasin D.

Electrophysiology

Only spontaneously beating single cardiomyocytes were selected for patch clamp recordings as previously described (Ji et al., 1999; Viatchenko-Karpinski et al., 1999). Whole cell or perforated patch measurements yielded similar results. Depolarizing pulses lasting 20 or 50 ms were applied at a frequency of 0.33 and 0.2 Hz, respectively, with an Axopatch 200-A (Axon Instruments, Inc.) or an EPC-9 amplifier (Heka). For most recordings, currents were leak subtracted using a P/n leak subtraction protocol (trace in Fig. 3, not leak subtracted). Data were acquired at a sampling rate of 2–10 kHz, filtered at 1 kHz, stored on hard disk, and analyzed offline using the ISO2 (MFK) or Pulse/Pulse-Fit (Heka) software package. Analysis of the (CCh) and the ISO effects was performed as previously described. Only those cells exhibiting a change in I_{Ca} density of >5% after ISO or CCh application were analyzed. The GTP-γ-S effect was compared with the response of untreated cells on the same experimental day. The average change in I_{Ca} density was calculated during the period of 180 s after break in (wt, $n = 9$; β1 integrin$^{-/-}$, $n = 10$; rescue cardiomyocytes, $n = 5$) and subtracted from the GTP-γ-S response.

$I_{K,ACh}$ recordings were made with equimolar K^+ concentrations to increase current amplitudes and GTP-γ-S (0.3 mM) in the pipette. Voltage ramp depolarizations (150 ms, −100–80 mV) were applied at a frequency of 0.1 Hz immediately after break in. Control ramp currents obtained before current activation were subtracted from $I_{K,ACh}$ currents, which were evident 1–2 min after membrane rupture. All currents were recorded from cells adhered to glass cover slips in a temperature-controlled (35°C) recording chamber. For I_{Ca}, the internal solution contained 120 mM CsCl, 3 mM $MgCl_2$, 5 mM MgATP, 10 mM EGTA, 5 mM Hepes, pH 7.4 (adjusted with CsOH), the external solution contained 120 mM NaCl, 5 mM KCl, 3.6 mM $CaCl_2$, 20 mM TEA-Cl, 1 mM $MgCl_2$, 10 mM Hepes, pH 7.4 (adjusted with TEA-OH). For $I_{K,ACh}$, the internal solution contained 40 mM KCl, 100 mM kaspartate, 5 mM MgATP, 2 mM EGTA, and 10 mM Hepes (pH adjusted to 7.4 with KOH), and the extracellular solution contained 140 mM KCl, 2 mM $MgCl_2$, 5 mM NaCl, 1.8 mM $CaCl_2$, 5 mM glucose, and 5 mM Hepes (pH adjusted to 7.4 with KOH). For perforated patch clamp recordings, amphotericin B (Sigma-Aldrich) was dissolved in DMSO and used at a final concentration of 250–500 μg/ml. Current measurements were initiated after the series resistance reached 10–20 MΩ. All substances were obtained from Sigma-Aldrich.

Data are expressed as mean ± SEM, paired or unpaired Student's *t* test was used to analyze electrophysiological data, and a p-value of <0.05 was considered significant.

Radioligand binding assays

EBs were harvested, and membrane homogenates were prepared. In brief, homogenates were incubated for 3 h at 22°C in 25 mM sodium phosphate (pH 7.4) containing 5 mM $MgCl_2$. Saturation binding experiments were carried out with (-)-[^{3}H]*N*-quinuclidinyl benzilate ([-]-[^{3}H]QNB; 42.0 Ci/mmol; NEN Life Science Products). Binding was performed with saturating concentrations of each radioligand (2 nM), and nonspecific binding was defined as binding in the presence of 2.5 μM atropine. Protein concentrations were determined by the Bradford method.

Immunocytochemistry

Whole EBs, EB and murine embryonic heart-derived isolated cells were incubated overnight with antibodies at 4°C. Antibodies included mouse anti–rat actinin (1:800; Sigma-Aldrich), monoclonal antitalin or antivinculin (1:100; Chemicon International), polyclonal rat anti–mouse β1 integrin (Sigma-Aldrich), rabbit polyclonal anti-M2 receptor (1:2,000; R&D Systems), α1C (1:200; Alomone Labs), and anti–G protein α-subunits. G protein antibodies against $G\alpha_{i1-3}$, $G\alpha_o$, and $G\alpha_s$ subunits (Santa Cruz Biotechnology, Inc.) were used at a 1:500 dilution. Next, cells were stained with Cy3- (or Cy2-) conjugated goat anti–rabbit (or goat anti–mouse) Ig (1:800, Sigma-Aldrich) and with a biotinylated goat anti–mouse (or anti–rabbit) IgG (1:400, Dako) or a biotinylated anti–rat antibody (Amersham Pharmacia Biotech) followed by streptavidin-conjugated Alexa FluorTM488 (1:200; Mo Bi Tec), streptavidin-conjugated Cy2 (1:100, Amersham Pharmacia Biotech), or Cy3 (1:600, Amersham Pharmacia Biotech).

Morphological analysis

The distribution pattern of $G\alpha_i$ was analyzed by fluorescence microscopy (ZEISS) in wt (EDS, 7 + 3; LDS, 7+11), β1 integrin$^{-/-}$ (EDS, 6 + 10; LDS, 6 + 14), and murine embryonic cardiomyocytes (E11.5/12.5, E17.5). All cardiomyocytes, identified by α-actinin costaining were analyzed on each slide (ranging from 49 to 174). Statistical analysis was performed using the unpaired Student's *t* test. DIC pictures were taken using an appropriately equipped Axiovert 135 microscope (ZEISS).

Deconvolution microscopy

For each specimen, an image stack (64 planes) was collected using an inverted ZEISS Axiovert 100 M with a ZEISS 63 Planapochromat oil immersion objective. Bandpass filter sets for Cy2 and Cy3 (AHF) without overlap in the fluorescence emission spectrum were used. The thickness of each optical section was 100 nm to assure appropriate optical resolution for the subsequent iterative deconvolution process. A three-dimensional deconvolution algorithm was applied to the image stacks (Schaefer, 1997) to increase the image resolution for colocalization (KS 400; ZEISS). Both theoretical point-spread functions (PSFs) based on microscope and specimen data and measured PSFs, calculated from fluorescent beads with a diameter of 1 μm (Molecular Probes, T-14792), were used. A conjugated gradient maximum likelihood deconvolution algorithm with 60 iterations was performed on the image stacks. Output intensities were scaled between gray value 0 and 255. Generally, theoretical and measured PSFs generated comparable results with slightly higher resolution in the resulting images by using the measured PSFs.

Immunogold labeling

Adult and embryonic mouse or rat heart tissue was perfused with 4% PFA in 0.1 M PBS or with 2% PFA/2% glutardialdehyde at 4°C. After fixation, the tissue was embedded with araldit or LR-white. The tissue grids were treated with 50 mM TBS for 15 min and blocked with 4% BSA in TBS for 1 h at room temperature. Then, primary antibodies against vinculin or talin (1:30–50) or β1 integrin (1:100; PharMingen) and a rabbit polyclonal antibody for $G\alpha_i$ were used at room temperature for 2 h. Grids were rinsed four times with 0.05% Tween-20–TBS, incubated with 5-nm gold-conjugated anti–mouse (or anti–rabbit) IgG (1:30–50) for 1 h, and treated with biotinylated goat anti–rabbit or anti–mouse (1:50; Dako) for 1 h at room temperature. Finally, specimens were incubated with 15-nm gold-labeled streptavidin (1:30; Zymed Laboratories) for 1 h followed by 2% glutardialdehyde fixation for 10 min. For contrast, grids were treated with 2% uranylacetate in 70% ethanol for 20 min and PBS for 7 min.

The authors thank Dr. A.M. Wobus for supplying wt ES cells of the line D3; M. Bickel, C. Böttinger, and B. Hops for assistance in cell culture work; C. Hoffmann, E. Janssen, and M. Reiner for their help in the ultrastructural studies; P. Sasse for taking the DIC pictures; and L. Schaefer and H. Bauch (ZEISS) for their support regarding deconvolution microscopy. We also thank Dr. N. Lenka and Dr. B. Nürnberg for helpful discussions and for critically reading the manuscript and A. Helmbold and Dr. B. Freedman for improving the writing of the manuscript.

This work was supported by a Deutsche Forshungsgemeinschaft grant (AD 54/2-1).

Submitted: 5 March 2001
Revised: 27 June 2001
Accepted: 28 June 2001

References

Anderson, R.G. 1998. The caveolae membrane system. *Annu. Rev. Biochem.* 67: 199–225.

Bloch, W., E. Forsberg, S. Lentini, C. Brakebusch, K. Martin, H.W. Krell, U.H. Weidle, K. Addicks, and R. Fassler. 1997. β1 integrin is essential for teratoma growth and angiogenesis. *J. Cell Biol.* 139:265–278.

Chen, F., K. Spicher, J.M. Jiang, L. Birnbaumer, and G.T. Wetzel. 2001. Lack of muscarinic regulation of Ca^{2+} channels in G(i2)α gene knockout mouse hearts. *Am. J. Physiol. Heart Circ. Physiol.* 280:H1989–H1995.

Clark, E.A., W.G. King, J.S. Brugge, M. Symons, and R.O. Hynes. 1998. Integrin-mediated signals regulated by members of the rho family of GTPases. *J. Cell Biol.* 142:573–586.

Diverse-Pierluissi, M., W.E. McIntire, C.S. Myung, M.A. Lindorfer, J.C. Garrison, M.F. Goy, and K. Dunlap. 2000. Selective coupling of G protein βγ complexes to inhibition of Ca^{2+} channels. *J. Biol. Chem.* 275:28380–28385.

Doetschman, T.C., H. Eistetter, M. Katz, W. Schmidt, and R. Kemler. 1985. The in vitro development of blastocyst-derived embryonic stem cell lines: formation of visceral yolk sac, blood islands and myocardium. *J. Embryol. Exp. Morphol.* 87:27–45.

Fanning, A.S., and J.M. Anderson. 1999. PDZ domains: fundamental building blocks in the organization of protein complexes at the plasma membrane. *J. Clin. Invest.* 103:767–772.

Fassler, R., M. Pfaff, J. Murphy, A.A. Noegel, S. Johansson, R. Timpl, and R. Albrecht. 1995. Lack of β1 integrin gene in embryonic stem cells affects morphology, adhesion, and migration but not integration into the inner cell mass of blastocysts. *J. Cell Biol.* 128:979–988.

Fassler, R., J. Rohwedel, V. Maltsev, W. Bloch, S. Lentini, K. Guan, D. Gullberg, J. Hescheler, K. Addicks, and A.M. Wobus. 1996. Differentiation and integrity of cardiac muscle cells are impaired in the absence of β1 integrin. *J. Cell Sci.* 109:2989–2999.

Fleischmann, M., W. Bloch, E. Kolossov, C. Andressen, M. Muller, G. Brem, J. Hescheler, K. Addicks, and B.K. Fleischmann. 1998. Cardiac specific expression of the green fluorescent protein during early murine embryonic development. *FEBS Lett.* 440:370–376.

Han, X., I. Kubota, O. Feron, D.J. Opel, M.A. Arstall, Y.Y. Zhao, P. Huang, M.C. Fishman, T. Michel, and R.A. Kelly. 1998. Muscarinic cholinergic regulation of cardiac myocyte ICa-L is absent in mice with targeted disruption of endothelial nitric oxide synthase. *Proc. Natl. Acad. Sci. USA.* 95:6510–6515.

Hescheler, J., M. Tang, B. Jastorff, and W. Trautwein. 1987. On the mechanism of histamine induced enhancement of the cardiac Ca^{2+} current. *Pflugers. Arch.* 410:23–29.

Hibino, H., A. Inanobe, M. Tanemoto, A. Fujita, K. Doi, T. Kubo, Y. Hata, Y. Takai, and Y. Kurachi. 2000. Anchoring proteins confer G protein sensitivity to an inward-rectifier K^+ channel through the GK domain. *EMBO J.* 4:78–83.

Hirsch, E., A. Iglesias, A.J. Potocnik, U. Hartmann, and R. Fassler. 1996. Impaired migration but not differentiation of haematopoietic stem cells in the absence of β1 integrins. *Nature.* 380:171–175.

Ibarrondo, J., D. Joubert, M.N. Dufour, A. Cohen-Solal, V. Homburger, S. Jard, and G. Guillon. 1995. Close association of the α subunits of Gq and G11 G proteins with actin filaments in WRK1 cells: relation to G protein-mediated phospholipase C activation. *Proc. Natl. Acad. Sci. USA.* 92:8413–8417.

Imanaka-Yoshida, K., M. Enomoto-Iwamoto, T. Yoshida, and T. Sakakura. 1999. Vinculin, talin, integrin α6β1 and laminin can serve as components of attachment complex mediating contraction force transmission from cardiomyocytes to extracellular matrix. *Cell Motil. Cytoskeleton.* 42:1–11.

Janmey, P.A. 1998. The cytoskeleton and cell signaling: component localization and mechanical coupling. *Physiol. Rev.* 78:763–774.

Ji, G.J., B.K. Fleischmann, W. Bloch, M. Feelisch, C. Andressen, K. Addicks, and J. Hescheler. 1999. Regulation of the L-type Ca^{2+} channel during cardiomyogenesis: switch from NO to adenylyl cyclase-mediated inhibition. *FASEB J.* 13:313–324.

Jurevicius, J., and R. Fischmeister. 1996. cAMP compartmentation is responsible for a local activation of cardiac Ca^{2+} channels by β-adrenergic agonists. *Proc. Natl. Acad. Sci. USA.* 93:295–299.

Kleuss, C., J. Hescheler, C. Ewel, W. Rosenthal, G. Schultz, and B. Wittig. 1991. Assignment of G-protein subtypes to specific receptors inducing inhibition of calcium currents. *Nature.* 353:43–48.

Kleuss, C., H. Scherubl, J. Hescheler, G. Schultz, and B. Wittig. 1993. Selectivity in signal transduction determined by γ subunits of heterotrimeric G proteins. *Science.* 259:832–834.

Kolossov, E., B.K. Fleischmann, Q. Liu, W. Bloch, S. Viatchenko-Karpinski, O. Manzke, G.J. Ji, H. Bohlen, K. Addicks, and J. Hescheler. 1998. Functional characteristics of ES cell–derived cardiac precursor cells identified by tissue-specific expression of the green fluorescent protein. *J. Cell Biol.* 143:2045–2056.

Kostin, S., D. Scholz, T. Shimada, Y. Maeno, H. Mollnau, S. Hein, and J. Schaper. 1998. The internal and external protein scaffold of the T-tubular system in cardiomyocytes. *Cell Tissue Res.* 294:449–460.

Maltsev, V.A., G.J. Ji, A.M. Wobus, B.K. Fleischmann, and J. Hescheler. 1999. Establishment of β-adrenergic modulation of L-type calcium current in the early stages of cardiomyocyte development. *Circ. Res.* 84:136–145.

Redfern, C.H., P. Coward, M.Y. Degtyarev, E.K. Lee, A.T. Kwa, L. Hennighausen, H. Bujard, G.I. Fishman, and B.R. Conklin. 1999. Conditional expression and signaling of a specifically designed Gi-coupled receptor in transgenic mice. *Nat. Biotechnol.* 17:165–169.

Rudolph, U., K. Spicher, and L. Birnbaumer. 1996. Adenylyl cyclase inhibition and altered G protein subunit expression and ADP-ribosylation patterns in tissues and cells from Gi2 $\alpha^{-/-}$ mice. *Proc. Natl. Acad. Sci. USA.* 93:3209–3214.

Ruoslahti, E. 1997. Integrins as signaling molecules and targets for tumor therapy. *Kidney Int.* 51:1413–1417.

Sakmann, B., A. Noma, and W. Trautwein. 1983. Acetylcholine activation of single muscarinic K^+ channels in isolated pacemaker cells of the mammalian heart. *Nature.* 303:250–253.

Sarndahl, E., G.M. Bokoch, F. Boulay, O. Stendahl, and T. Andersson. 1996. Direct or C5a-induced activation of heterotrimeric Gi2 proteins in human neutrophils is associated with interaction between formyl peptide receptors and the cytoskeleton. *J. Biol. Chem.* 271:15267–15271.

Schaefer, L. 1997. Increased spatial resolution by using advanced restoration methods for microscopical data sets. *Bull. Microscop. Soc. Canada.* 3:19–25.

Short, S.M., J.L. Boyer, and R.L. Juliano. 2000. Integrins regulate the linkage between upstream and downstream events in G protein-coupled receptor signaling to mitogen-activated protein kinase. *J. Biol. Chem.* 275:12970–12977.

Sowell, M.O., C. Ye, D.A. Ricupero, S. Hansen, S.J. Quinn, P.M. Vassilev, and R.M. Mortensen. 1997. Targeted inactivation of αi2 or αi3 disrupts activation of the cardiac muscarinic K^+ channel, ik+ach, in intact cells. *Proc. Natl. Acad. Sci. USA.* 94:7921–7926.

Towbin, J.A. 1998. The role of cytoskeletal proteins in cardiomyopathies. *Curr. Opin. Cell Biol.* 10:131–139.

Trautwein, W., and J. Hescheler. 1990. Regulation of cardiac L-type calcium current by phosphorylation and G proteins. *Annu. Rev. Physiol.* 52:257–274.

Ueda, H., S. Saga, H. Shinohara, R. Morishita, K. Kato, and T. Asano. 1997. Association of the γ12 subunit of G proteins with actin filaments. *J. Cell Sci.* 110:1503–1511.

Vandecasteele, G., T. Eschenhagen, H. Scholz, B. Stein, I. Verde, and R. Fischmeister. 1999. Muscarinic and β-adrenergic regulation of heart rate, force of contraction and calcium current is preserved in mice lacking endothelial nitric oxide synthase. *Nat. Med.* 5:331–334.

Vasioukhin, V., C. Bauer, M. Yin, and E. Fuchs. 2000. Directed actin polymerization is the driving force for epithelial cell-cell adhesion. *Cell.* 21:209–219.

Viatchenko-Karpinski, S., B.K. Fleischmann, Q. Li, H. Sauer, O. Gryshchenko, G.J. Ji, and J. Hescheler. 1999. Intracellular Ca^{2+} oscillations drive spontaneous contractions in cardiomyocytes during early development. *Proc. Natl. Acad. Sci. USA.* 96:8259–8264.

Wang, Y.G., A.M. Samarel, and S.L. Lipsius. 2000a. Laminin acts via integrin signalling to alter cholinergic regulation of L-type Ca^{2+} current in cat atrial myocytes. *J. Physiol.* 526:57–68.

Wang, Y.G., A.M. Samarel, and S.L. Lipsius. 2000b. Laminin binding to 1-integrins selectively alters 1- and 2-adrenoceptor signalling in cat atrial myocytes. *J. Physiol.* 527:3–9.

Wickman, K., and D.E. Clapham. 1995. Ion channel regulation by G proteins. *Physiol. Rev.* 75:865–885.

Wobus, A.M., G. Wallukat, and J. Hescheler. 1991. Pluripotent mouse embryonic stem cells are able to differentiate into cardiomyocytes expressing chronotropic responses to adrenergic and cholinergic agents and Ca^{2+} channel blockers. *Differentiation.* 48:173–182.

Wu, X., J.E. Mogford, S.H. Platts, G.E. Davis, G.A. Meininger, and M.J. Davis. 1998. Modulation of calcium current in arteriolar smooth muscle by αv β3 and α5 β1 integrin ligands. *J. Cell Biol.* 143:241–252.

Ye, C., M.O. Sowell, P.M. Vassilev, D.S. Milstone, and R.M. Mortensen. 1999. Gα(i2), Gα(i3)and Gα(o) are all required for normal muscarinic inhibition of the cardiac calcium channels in nodal/atrial-like cultured cardiocytes. *J. Mol. Cell. Cardiol.* 31:1771–1781.